Neurotoxicology and Teratology 76 (2019) 106836

Contents lists available at ScienceDirect

Neurotoxicology and Teratology

journal homepage: www.elsevier.com/locate/neutera

A combination insecticide at sub-lethal dose debilitated the expression pattern of crucial signalling molecules that facilitate craniofacial patterning in domestic chick *Gallus domesticus*

Shashikant Sharma[a], Gowri K. Uggini[a], Isha Desai[b], Suresh Balakrishnan[a,*]

[a] Department of Zoology, Faculty of Science, The Maharaja Sayajirao University of Baroda, Vadodara 390002, Gujarat, India
[b] N. V. Patel College of Pure and Applied Sciences, Vallabh Vidyanagar, Anand 388120, Gujarat, India

ARTICLE INFO

Keywords:
Craniofacial malformation
Combination insecticide
Chick embryo
BMP
WNT
SHH

ABSTRACT

Pesticides despite being agents that protect the plants and humans from noxious pests, are infamous for their potential to cause detrimental health issues in nontargeted species. In order to ascertain the latter, a set of experiments were conducted by exposing early chick embryos to a widely used combination insecticide (Ci, 50% chlorpyrifos and 5% cypermethrin). The results revealed a myriad of congenital defects pertaining to craniofacial development such as anophthalmia, microphthalmia, exencephaly as well as deformed beak and cranial structures. These teratological manifestations could be attributed to the Ci induced alteration in the titre of major regulators of neurulation and ossification. Therefore, the mRNA and/or the protein level expression pattern of genes which are reported to be involved in the craniofacial development were studied at selected time points of embryonic development. The analysis of the result showed that there have been significant alternations in the expression patterns of the signalling molecules such as SHH, WNTs, CDH1, CDH2, L1CAM, PAX6, HOX, PCNA, GLI3, BMP7, FGF8, GLIs, SOX9, RUNX2, DLX5, COL10A1, CASPASE3 etc. on embryonic days 2, 4 and/or 10. Concurrently, on day 10, whole-mount skeletal staining and biochemical estimation of hydroxyproline were carried out in the cranial tissues of the embryos. The overall result of the current study indicates that exposure to Ci during early development impede the crucial regulatory signals that orchestrate the morphogenesis of cranial neural crest cells thereby hindering the normal progression of neural tube and endochondral ossification which collectively lead to craniofacial dysmorphism in domestic chicks.

1. Introduction

The mystery behind the embryonic development was a reason enough to initiate a series of studies spanning several years by the leading laboratories across the world. Many fundamental questions on development were unearthed using animal models such as *Drosophila*, *C. elegans*, *Xenopus*, chick and mouse. But the chick still remains as a popular vertebrate model since the genome of chick have considerable homology with human and hence, unlike a murine model, finer mechanisms of development can be studied without causing any harm to the mother (Abdul-Ghani et al., 2012). However, the normal embryonic development is often disturbed due to exposure to various stressors at a critical stage of embryogenesis resulting in developmental anomalies. Some of the known factors that can induce congenital abnormality include temperature, hypoxia, UV rays, free radicals and pesticides (Kalliora et al., 2018). Out of these, man-made chemicals, mainly pesticides are of a special concern due to its widespread usage in day to day life.

In the recent past increase in the frequency of pesticide induced neural tube malformation has been reported (Wang et al., 2017). Moreover, the neural tube defects (NTDs) are reported to be more common than any other congenital defects, affecting over 300,000 births every year (NCBDDD, 2012). These anomalies relate to the disturbances in normal growth and development of the brain, spine and other essential craniofacial structures. Against this backdrop our lab has conducted a series of teratological screening of one of the most widely used insecticide combination (Chlorpyrifos 50% + Cypermethrin 5%) in chick. The result showed widespread malformations in the hatchlings of combination insecticide (Ci) treated eggs like distorted cephalization, anophthalmia, wry neck, craniorachischisis, diprosopus and ventral body wall defects (Uggini et al., 2012; Uggini and Suresh, 2013; Sharma et al., 2018). Interestingly, even though, there are ample evidences

* Corresponding author.
E-mail addresses: uggini.gowri-zoo@msubaroda.ac.in (G.K. Uggini), b.suresh-zoo@msubaroda.ac.in (S. Balakrishnan).

https://doi.org/10.1016/j.ntt.2019.106836
Received 19 June 2019; Received in revised form 4 September 2019; Accepted 11 September 2019
Available online 05 October 2019
0892-0362/

suggesting the teratogenic potential of these two pesticides as individual entities (Ahmed, 2007; Slotkin et al., 2008), a concerted effort to understand the synergistic action of this combination of insecticide in inducing developmental anomalies is scanty to the best our knowledge. Nonetheless, both the pesticides are reported to act in synergy to augment the toxic manifestations (Ray and Forshaw, 2000). Therefore, we hypothesise that multiple developmental facets would be under the negative effects of Ci and hence, an attempt was made to elucidate the molecular mechanisms behind one of the most frequently encountered developmental abnormalities observed in the Ci treated chick embryos – the craniofacial malformation.

It has been documented that the key processes in craniofacial development include the formation of cranial neural crest (CNC), via induction, specification, delamination and migration, followed by its morphogenesis and histogenesis (Fish, 2016). The above-mentioned events are suggested to be tightly regulated by several gene products or genetic factors which coordinate for craniofacial formation and patterning. These factors include many signalling molecules viz. SHH, FGFs, BMPs, and WNTs which orchestrate the complex cellular processes such as cell adhesion, migration, proliferation and apoptosis (Suzuki et al., 2016). Nonetheless, depending on the time of embryonic development and location in the embryo, their expression becomes critical in deciding the fate of cell (Yang and Ornitz, 2019). Therefore, in the current study in order to deduce the effect of Ci on the signalling molecules that facilitate the sequential development of craniofacial structures, chick embryos of three different developmental stages namely Hamburger and Hamilton (HH) stage 13, 24 and 36 (corresponding to days 2, 4 and 10 of embryonic development) were selected (Hamburger and Hamilton, 1951). The day 2 embryo is characterized by the presence of primary optic vesicles and well-established optic stalk along with a distinct telencephalon and forebrain covered with head fold of amnion. However, distinct eye pigmentation and enlargement of head structures can be observed by day 4. On day 10, primary calcification of the body begins which extends towards the remaining cartilaginous area until the hatching (Sawad et al., 2009). The selected stages therefore, help in understanding the levels of few key molecular signals involved in neural tube patterning and endochondral ossification during early stages of chick embryonic development upon *in ovo* exposure of combination insecticide.

2. Materials and methods

2.1. Toxicant

The test article formulation constituted of a mixture of chlorpyrifos (50%) and cypermethrin (5%). It is commercially retailed as Anaconda 505™ manufactured by AIMCO Pesticides Limited, Mumbai, India.

2.2. Test system

Fertilized eggs from Rhode Island Red (*Gallus domesticus*) breed of domestic chicken were used in the study and were procured from the Intensive Poultry Development Unit, Vadodara, India. The experimental protocols were in full compliance with the guidelines of Drugs and Cosmetics Rules 1945, Appendix-III animal care standard and were approved by the institutional animal ethics committee (Protocol number: IAEC 84/08/2014-2) in accordance with the norms of the committee for the purpose of control and supervision of experiments on animals (CPCSEA), India.

2.3. Experimental design

The eggs were divided at random into control and treatment groups after properly disinfected with 0.5% povidone iodine solution. With the help candling method, air space was marked with the pencil and later the eggshell was punctured on day “0” of incubation, with a fine needle (Blankenship et al., 2003). Olive oil (Figaro, India) was injected in the control groups whereas the treatment group was administered with sublethal dose (0.05 µg per egg) of pesticide solution with olive oil as vehicle. Previous work from the lab aided to choose the ideal dosage for the study (Uggini et al., 2012). The whole procedure was strictly carried out in sterile condition in the laminar air hood to avoid any contamination. All the experimental eggs were kept with their broad ends facing upwards in an automated incubator (Scientific equipment works, New Delhi) at a temperature of 37.5 °C ± 0.5 and relative humidity of 70–75%. The eggs were automatically rotated every hour and were checked for mortality every two days till the day of sample collection.

2.4. Embryo collection

The eggs were cracked opened with the help of a scalpel and subsequently checked for the Hamilton-Hamburger (HH) stages of chick development. The embryos that had reached HH stage 13 (day 2), HH stage 24 (day 4) and HH stage 36 (day 10) were only collected for the study.

2.5. Rate of mortality and malformations

The embryos were collected at day 2, day 4 and day 10 of incubation. The rate of mortality and malformations was recorded on all three stages. In day 10 embryos, the size of the head (head breadth) was also measured with the help of Vernier calliper (Mitutoyo Corporation, Japan). The experiment was performed thrice with 30 eggs in each group (control and treatment) each time.

2.6. Real time RT-PCR

The chick embryos were isolated and rinsed with cold PBS. Head region was specifically dissected out from control and treatment groups and was homogenized using TRIzol reagent (Applied Biosystems, USA) for total RNA isolation. cDNA was synthesized using one step cDNA synthesis kit procured from Applied Biosystems, USA. As per the recommended protocol, only 1 microgram of total RNA was used for cDNA synthesis. The primer sequences used in the study were obtained from NCBI and are listed in Table 1. Quantitative RT-PCR was performed using Lightcycler96 (Roche Diagnostics, Switzerland). The following program was set for the reaction to be carried out: denaturation for 100 s at 95 °C, 42 cycles of amplification (10s at 95 °C, 30s at 60 °C,

Table 1
Oligonucleotide primers used for RT-PCR analysis.

Gene	Forward primer	Reverse primer
SHH	TGCTAGGGATCGGTGGATAG	ACAAGTCAGCCCAGAGGAGA
WNT5	GACACTTGGCAGCACAATGG	CCCTAGAGACCACCAAGAGC
CDH1	GAAGACAGCCAAGGGCCTG	TCTGGTACCCCTACCCTCTTG
WNT7	TATCGTCATCGGGGAAGGGT	GCTGCTTCTCTGCTACCCAC
CASPASE3	AAAGATGGACCACGCTCAGG	TGACAGTCCGGTATCTCGGT
L1CAM	TTCCCCCGGAGTATGGTGC	CTGGGGAAGACCACGAGTTG
FGF8	GAGACCGACACCTTTGGGAG	TTGCCGTTACTCTTGCCGAT
CDH2	AGCCCACGGAGTTTGTAGTG	TTTGGTCCTTTTCTGAGGCCC
BMP7	ATCTGCCTACAAAATTGGTTCTC	TACTCACAGCGCATTCTCACTT
PCNA	TGTTCCTCTCGTTGTGGAGT	TCCCAGTGCAGTTAAGAGCC
BMP2	ATGTTGGACCTCTATCGCCTG	CCAAAACTTCTTCGTGGTGG
FGF2	ATCCGGGAGAAAAACGACCC	TTGGTCGTCTCGCTCCAAAC
GLI3	TCTCGTAGCAGTTCGTCAGC	TCAGAGCAGGGCTTATTGCG
GLI2	GGGGATGGCTTTACGGAGAC	CAATGGAGGAGGCCCGTG
WNT1	AAGTCGGGAAGGAGAGGTGA	GAGCCATCTGAAACTGCCCT
HOX10a	GAGCCCGTAGGCAATTCAAA	ACGCTCACGAGTCAGGTACA
HOX11a	CAGCTCCAGTGGACAACGG	GAGCTGGAGGCGTTTCTCTT
PAX6	AGCAAGGATACAGGTGTGGT	TGTGGGATCGGCTGGTAAAC
SOX9	CAGACGCACATCTCTCCGAA	TCCCTGTGACTGACCCGAAT
RUNX2	CTGGTGCCTTTTGGGTTGTG	TCGACACGTCTTGCTTAGCG
DLX5	GGAATGCGGATGGGGGATTT	CCACAGCTGAGCCGAAAAAC
18S rRNA	GGCCGTTCTTAGTTGGTGGA	TCAATCTCGGGTGAAC

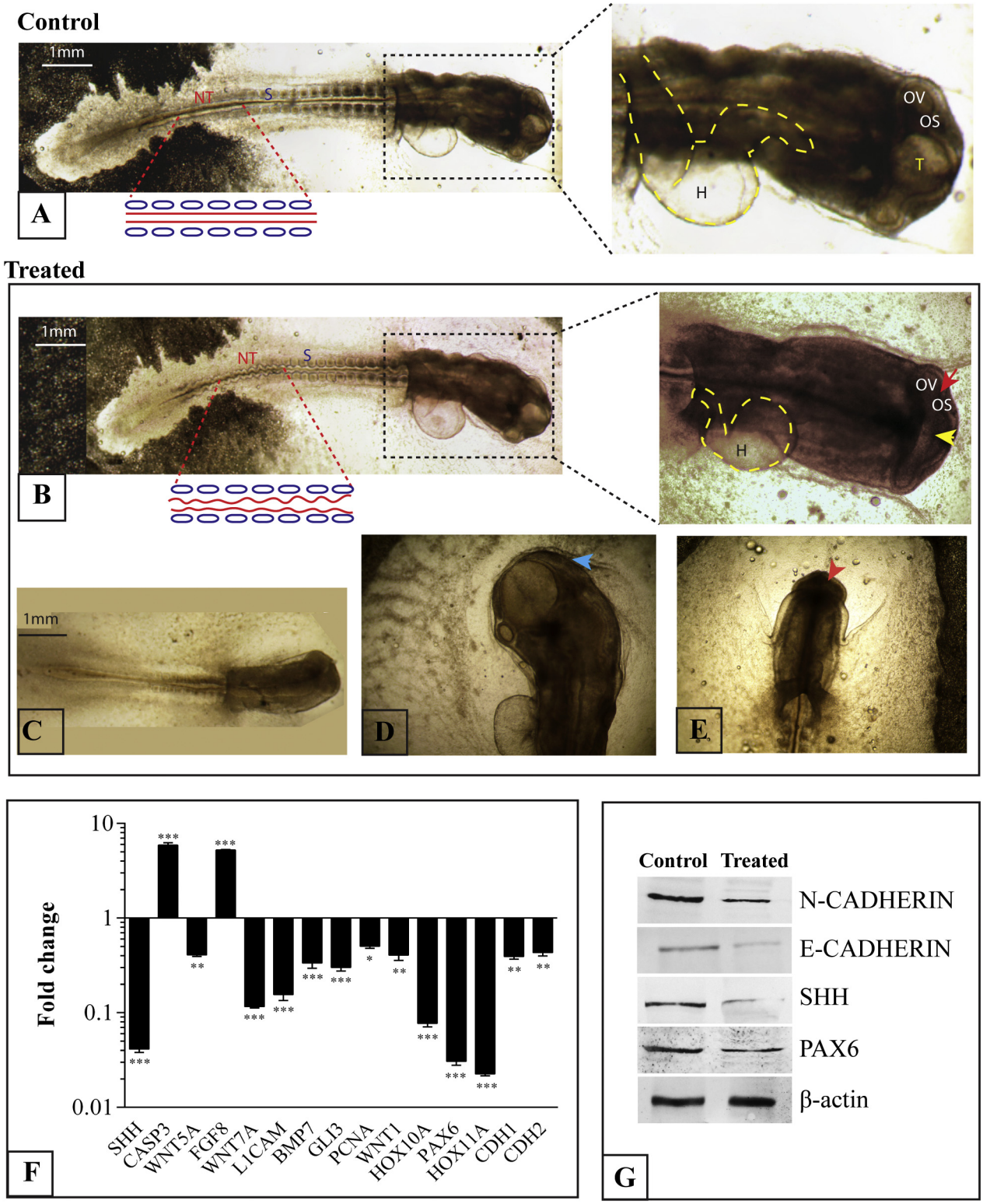

Fig. 1. Pesticide induced structural defects: (A) control embryo of day2 with well-developed optic vesicles (OV), optic stalk (OS), telencephalon (T), S-shaped heart (H), somites (S) and neural tube (NT); (B) Ci treated day 2 embryo with under developed optic stalk (red arrowhead), telencephalon (yellow arrowhead),irregular heart shape (yellow dotted line) and wavy neural tube (NT); (C) Ci treated embryo showing reduction in size (Scale = 1 mm); (D) absence of eye stalk marked by blue arrowhead in Ci treated embryo; (E) underdeveloped telencephalon in treated embryo (red arrow head); (F) mRNA expression pattern of the genes involved in regulation of morphogenesis for Ci treated day 2 embryo. Values are expressed in fold change (Mean ± SEM). Fold change values for control embryo is 1.0 for all the genes (*: $p \leq 0.05$; **: $p \leq 0.01$; ***: $p \leq 0.001$); (G) Western Blot image showing comparative expression of various proteins: E-CADHERIN, N-CADHERIN, SHH, PAX6 on day 2. β-Actin was taken as loading control, (n = 3).

Table 2
Mortality observed on day 2, 4 and 10 of embryonic development in control and combination insecticide treated groups. The values are expressed as mode with range in parenthesis; n = 3 with 30 eggs per group per day.

Group	Number of dead embryos		
	Day 2	Day 4	Day 10
Control	4 (2,6)	4 (3,7)	5 (2,5)
Treated	12 (9,13)***	9 (8,12)***	12 (10,16)***

*** $p \leq 0.001$.

30s at 72 °C. To confirm the specific product formed by the reaction mixture, melt curve analysis and gel electrophoresis were performed. After the analysis, fold change was calculated and represented as $2^{-\Delta\Delta Cq}$ according to Livak and Schmittgen (2001). 18SrRNA was used as an endogenous control. In order to minimise biological variation, the tissue samples from three embryos were pooled and for each variable analysed in RT-PCR, three technical replicates were performed to reduce the experimental error.

2.7. Protein expression analysis

Tissues (only head region) were collected on day 2, 4 and 10 from both control and treatment groups. For each day, tissues from three embryos were pooled and homogenized in Tris-SDS lysis buffer with protease inhibitor (Sigma Aldrich, USA). Moreover, for each protein studied the experiments were repeated thrice to minimise experimental error. 10% homogenates were assayed for total protein content by Bradford method (1976). Equal amount of total protein was loaded and separated by SDS-PAGE on 10% gels. Protein was transferred onto nitrocellulose membrane by semi-dry transfer at 100 mA for 30 min. The membrane was probed separately with antibodies against 0.1 µg/ml of anti-SHH IgG Mouse, anti- Cl. CASPASE3 IgG Rabbit, anti-PAX6 IgG Mouse, anti-*E*-CADHERIN IgG Mouse, anti-N-CADHERIN IgG Mouse, anti-BMP2 IgG Mouse and anti-β-Actin IgG Mouse. The blot was developed by ALP, BCIP-NBT system (Sigma-Aldrich, USA).

2.8. Hydroxyproline estimation

The tissues from the cranial region of day 10 control and experimental groups were excised and three such samples from each group were pooled to estimate the hydroxyproline content, as described by Edwards and O'Brien Jr (1980). The experiments were repeated thrice for statistical conclusion. The samples were first dried and then acid hydrolysed at 120 °C in a pressure vessel for 2–4 h. Upon completion of hydrolysis, hydrolysates and standards tubes were kept in oven at 60 °C for 8 h for complete evaporation of water. The homogenates and standards were added to 1.5 ml tubes, along with the same volume of citric/acetate buffer of pH 6.0 (citric acid, sodium acetate, sodium hydroxide, glacial acetic acid, n-propanol) and chloramine-T solution (chloramine-T dissolved in Milli-Q water). The tubes were incubated for 20 min at room temperature and Ehrlich's solution (*p*-dimethyl-amino benzaldehyde, perchloric acid and n-propanol) was added to the tubes which were then incubated at 60 °C for 15 min. The absorbance of the reaction product was read at 550 nm. The amount of hydroxyproline in each sample was calculated using regression curve of standard graph.

2.9. Alcian blue and alizarin red staining

Ten embryos were collected at day 10 for visualizing the skeletal impairments. The embryos from both the groups were fixed in 4% paraformaldehyde and later washed in PBS for 2–3 days. These samples were stained for 6 h in dark condition at room temperature with a filtered (0.1%) Alcian blue and (0.1%) Alizarin red solution (in 30% acetic acid and 70% ethanol) and dehydrated in 95% ethanol for an hour. The tissues were then washed under tap water for 2 h and afterwards transferred to 1% potassium hydroxide solution for 2 h. These samples were destained in a graded sequence of glycerol and potassium hydroxide and finally stored in 100% glycerol at 4 °C (Depew, 2008).

2.10. Statistical analysis

The data for mortality and malformations are represented as Mode with Range as variability and were analysed for statistical significance by Mann-Whitney *U* Test. The rest of the linear data were analysed by two-tailed Student's *t*-test using Prism v5.03 (GraphPad Software Inc., USA) and are expressed as Mean ± Standard Error of Mean. *p* value less than or equal to 0.05 was considered as statistically significant.

3. Results

3.1. Day 2

The control group embryos on day 2 (HH stage 12) showed characteristic features of the left profile of the head like clearly demarcated telencephalon, well established optic vesicles and optic stalk as well as S-shaped heart (Fig. 1A). On the other hand, the embryos from the treatment group exhibited overt signs of toxicity with respect to craniofacial development. Moreover, the rate of occurrence of malformations as well as mortality was significantly higher in the treated group (Tables 2, 3). The aberrations such as underdeveloped heart (Fig. 1B), reduction in size of the whole embryo (Fig. 1C), absence of eye stalk (Fig. 1D) and underdeveloped telencephalon (Fig. 1E) were frequently encountered in the Ci treated embryos. In addition, an interesting feature of wavy neutral tube, was noticed in the embryos from treatment group (Fig. 1B). In order to ascertain the reason behind the malformations cited above, certain signalling molecules, which are known to regulate the patterning of cranial features, were studied at mRNA and protein expression levels. The mRNA levels of genes which play a major role in the dorso-ventral patterning of neural crest cells viz., SHH, WNT7A, BMP7, GLI3, WNT5A and WNT1 showed significant reduction in the embryos treated with Ci. However, the transcript levels of genes involved in the anteroposterior patterning exhibited aberrant expression pattern in response to Ci challenge. While the levels of HOX10A, HOX11A and PAX6 transcript got downregulated, FGF8 mRNA level was found upregulated in the treated embryos compared to the controls. The relative mRNA expression levels of the genes which bring about the closure of the neural tube namely CDH1, CDH2 and L1CAM have also shown significant reduction in response to Ci treatment (Table 4; Fig. 1F). Furthermore, expression of CASPASE3, a marker for apoptosis, was found upregulated in the embryos subjected to Ci (Table 4; Fig. 1F). A concomitant, immunoblot analysis for protein revealed reduced expressions of SHH, PAX6, E-CADHERIN and N-CADHERIN in the treated embryos on day 2 compared to the control embryos (Fig. 1G). The band intensity of SHH, PAX6, E-CADHERIN and N-CADHERIN were analysed in the representative blots (n = 3) and the result revealed noteworthy reduction in the Ci group with respect to controls (Table 7).

Table 3
Malformations observed on day 2, 4 and 10 in live embryos. The values are expressed as mode with range in parenthesis; n = 3 with 30 eggs per group per day.

Group	Number of malformed embryos		
	Day 2	Day 4	Day 10
Control	0 (0,1)	0 (0,2)	2 (0,2)
Treated	9 (9,13)***	14 (11,15)****	12 (10,14)***

*** $p \leq 0.001$.
**** $p \leq 0.0001$

Table 4
mRNA expression pattern of the genes involved in regulation of morphogenesis of Ci treated day 2 embryo. Fold changes are expressed as Mean ± SEM. Fold change values for control embryo is 1.0 for all the genes, n = 3 with 30 eggs per group per day.

Gene expression	Fold change (mean ± SEM)
SHH	0.041406 ± 0.003***
CASPASE3	5.89 ± 0.340***
WNT5A	0.4081 ± 0.014**
FGF8	5.249248 ± 0.039***
WNT7A	0.116231 ± 0.004***
L1CAM	0.155403 ± 0.020***
BMP7	0.335943 ± 0.042***
GLI3	0.301888 ± 0.025***
PCNA	0.533664 ± 0.024*
WNT1	0.406431 ± 0.049**
HOX10A	0.077208 ± 0.006***
PAX6	0.030711 ± 0.002***
HOX11A	0.022543 ± 0.001***
CDH1	0.393014 ± 0.025**
CDH2	0.433156 ± 0.035**

* $p \leq 0.05$.
** $p \leq 0.01$.
*** $p \leq 0.001$.

3.2. Day 4

On day 4 (HH stage 24), treated group showed significant increase in the rate of mortality (Table 2) as well as incidences of malformations (Table 3). The control group showed normal development with distinct optic cup, eye pigmentation, limb buds and allantois formation (Fig. 2A). Visual examination of treated embryos showed defects like anophthalmia, reduced allantois and stunted growth (Fig. 2B). Moreover, brain lobes like telencephalon, mesencephalon and metencephalon were reduced in size as compared to control embryos (Fig. 2B).

To unearth the molecular mechanism behind these malformations observed in treated embryo, key signalling molecules involved in neural crest cell patterning, proliferation and cell death were investigated at transcript and protein level. Relative mRNA expression levels in day 4 treated embryos exhibited remarkable downregulation of SHH, WNT5A, L1CAM, GLI3, WNT1, HOX10A, HOX11A, PAX6, CDH1 and CDH2 genes. While the PCNA and WNT7A transcript levels were conspicuously reduced ($p \leq 0.01$) in the treated embryos. The change in expression level of BMP7 however, was found statistically insignificant. On the contrary, qRT-PCR analysis of CASPASE3 and FGF8 transcripts revealed appreciable hike in their expression (Table 5; Fig. 2C). Western blot results for CASPASE3 and SHH were in agreement with their respective gene expression levels (Fig. 2D, Table 7).

3.3. Day 10

Significant increase in the rate of mortality (Table 2) as well as occurrence of malformations (Table 3) was noted in treatment group of day 10 (HH stage 36) embryo. The control set of embryos (Fig. 3A) on day 10 showed usual development of head, well defined beak and visceral organ. The embryos from treatment group showed exposed brain (Fig. 3B), unilateral anophthalmia and phocomelia (Fig. 3C), bilateral anophthalmia (Fig. 3D), absence of beak (Fig. 3E) and exposed visceral organs (Fig. 3B–E). Also, the result of the morphometric analysis on the day 10 embryo embryos revealed a significant reduction in the head breadth in treatment group compared to control (Table 8).

Further, the relative mRNA expressions of the genes involved in chondrogenesis, i.e. chondrocyte proliferation as well as differentiation, was studied in the cephalic tissues to understand the degree of maturation of skeletal elements. The Ci dosed embryos showed a considerably diminished expression of SOX9, COL10A1, BMP7, WNT5A and RUNX2, whereas CASPASE3 and FGF8 mRNA levels were found amplified. No noticeable changes were seen in case of DLX5, FGF2, GLI3 and GLI2 gene expression (Table 6; Fig. 3F). The samples extracted from day 10 embryos subjected to Ci showed reduced expressions of SHH and BMP2 at both gene and protein levels (Tables 6, 7; Fig. 3F, G).

Additionally, the extent of chondrogenesis was checked through differential staining of cranial region in day 10 chick embryos by Alcian blue (stains cartilage) and Alizarin red (stains bone). It was evident from the results that there is a marked reduction in endochondral ossification in the cranial region of the Ci treated embryos (Fig. 3I). Alizarin red stained bones of lower jaw exhibited an incomplete fusion as well as partial ossification in treated embryos as opposed to the control ones (Fig. 3H). Moreover, upon removal of eyeball from embryos, the interorbital sinus in treated embryo, illustrated hampered chondrogenesis in contrast to embryos of control group. The extent of ossification of pre-maxilla and maxilla bones (involved in beak formation) was also reduced in treated embryos (Fig. 3I). The results obtained by Alcian blue-Alizarin red staining was further reaffirmed by biochemical estimation of hydroxyproline, which is a major structural protein found in the cartilage. A sharp drop was observed in hydroxyproline content in treated group as compared to that of control embryos on day 10 (Fig. 3J) hence, reiterating the results of mRNA, protein and histological studies mentioned previously.

4. Discussion

The ominous danger of insecticide intoxication during development is extremely worrisome since a brief exposure during the critical window of embryonic development can cause highly distressing morphological and anatomical anomalies. We tried to understand the possible alterations in the signalling pathways during the early embryogenesis which might have led to the observed craniofacial dysmorphism provoked by combination insecticide exposure. Much of the embryonic dysmorphs observed here could be attributed to the lapses in the process of neurulation. The primary neurulation is of prime importance in the development of chick embryo, in which the two sides of flat neural plate begin to converge and involute at the midline and adhere to each other to form the neural tube (Gilbert, 2003). Any failure in this closure towards the rostral and/or caudal end, results in conditions like anencephaly and/or spina bifida respectively, and if the tube fails to fuse throughout the body it would lead to rachischisis. The present study reveals such defects in neural tube closure on day 2 in the pesticide treated embryos. Hence, we looked into the molecular regulators of these embryonic events.

The chick embryo expresses E-cadherin and L1-CAM throughout the ectoderm during the neurulation process (Taneyhill, 2016). These Ca^{2+} dependent cell adhesion molecules are the identity of the neuro-ectodermal plate and their expression regulates the fusion process. Due to the switch in gene expression, cells subsequently express N-Cadherin which pave way for the separation of ectodermal and non-ectodermal cell types (Taneyhill, 2016). Herein, our results showed downregulation in mRNA expression levels of E-cadherin (CDH1), N-cadherin (CDH2) and L1-CAM in the Ci treated embryos when compared to the control embryos on day 2 and 4. A concomitant immunoblot analysis reaffirmed the reduction in the expression of E-cadherin and N-cadherin at protein level as well in the Ci treated embryos. This dysregulation, especially in N-cadherin levels might have led to the improper closure of the neural tube, thereby disturbing the neurulation and causing anomalies in the rostral region of the embryos. Similar results were reported by Detrick et al. (1990) wherein deficiency of N-cadherin levels induced morphological defects in *Xenopus* embryos.

Further, as the surface ectoderm separates from the newly formed neural tube, a group of cells delaminate from its anterior most layer, undergo epithelial to mesenchymal transition and migration to further diversify into various cell types termed as cranial neural crest cells. These multipotent cells in the later stages of development give rise to

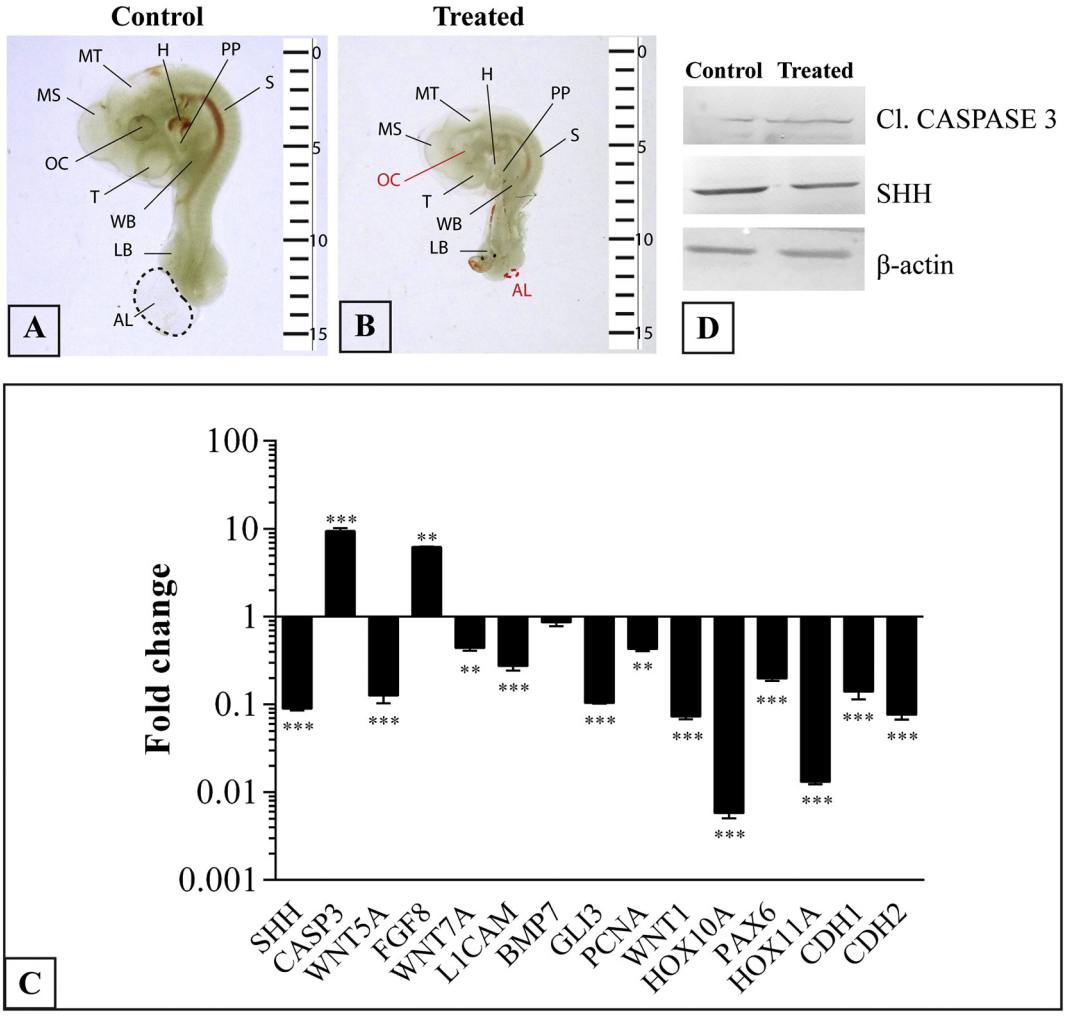

Fig. 2. Photograph of (A) day 4 Control embryo with well-developed structures indicating telencephalon (T), mesencephalon (MS), metencephalon (MT), optic cup (OC), pharyngeal pouch (PP), wing bud (WB), somites (S), leg bud (LB) and allantois (AL); (B) day 4 treated embryo with reduced allantois and absence of optic cup (marked by red coloured text). Scale in mm; (C) transcript level expression of genes involved in neural tube patterning in Ci treated day 4 embryos. Values are expressed in fold change (Mean ± SEM). Fold change values for control embryo is 1.0 for all the genes; (D) Western Blot images showing comparative expression of SHH and cleaved CASPASE3 on day 4. β-Actin was taken as loading control, (n = 3) (**: $p \leq 0.01$; ***: $p \leq 0.001$).

Table 5
Transcript level expression of genes involved in neural tube patterning in Ci treated day 4 embryos. Fold changes are expressed as Mean ± SEM. Fold change values for control embryo is 1.0 for all the genes; n = 3 with 30 eggs per group per experiment.

Gene expression	Fold change (mean ± SEM)
SHH	0.089 ± 0.004***
CASPASE3	9.415 ± 0.780***
WNT5A	0.126 ± 0.023***
FGF8	6.183 ± 0.048**
WNT7A	0.440 ± 0.029**
L1CAM	0.273 ± 0.030***
BMP7	0.863 ± 0.083
GLI3	0.103 ± 0.001***
PCNA	0.428 ± 0.024**
WNT1	0.073 ± 0.005***
HOX10A	0.006 ± 0.0007***
PAX6	0.197 ± 0.012***
HOX11A	0.013 ± 0.0007***
CDH1	0.140 ± 0.026***
CDH2	0.077 ± 0.009***

** $p \leq 0.01$.
*** $p \leq 0.001$

forebrain meninges, craniofacial cartilage, bones of the jaw, neurons and glia in the vertebrate embryo (Mayor and Theveneau, 2013). The formation of neural crest cells is a complex process carried out under the influence of micro-environment signals that confer patterning and migratory capabilities to this cell population (Nikolopoulou et al., 2017). Many paracrine factors such as SHH, WNTs, BMPs and FGFs, PAX6 are secreted from the adjacent tissues to induce patterning in the neural tube in a gradient fashion (Griffin et al., 2013). Depletion of neural crest cells or perturbations in the gene expressions during patterning process, have been reported in mouse models to cause neural tube defects, microphthalmia and reduced size or absence of jaw structures, suggesting their importance in the development of the future brain (Wilde et al., 2014).

The neural tube undergoes patterning along its two major axes, dorso-ventral (DV) and anterior-posterior (AP), to form a functional nervous system under the activities of paracrine factors secreted from ventral floor plate and dorsal roof plate. SHH cooperates with BMP7, to play an important role in patterning the dorso-ventral axis of the nervous system. Mutations in the SHH gene in mouse and humans have suggested its role to be critical around birth (Ahlgren and Bronner-Fraser, 1999). In addition, targeted deletion of SHH causes significant craniofacial defects such as holoprosencephaly and cyclopia (Xavier et al., 2016). Moreover, knockout studies of BMP7 in mice have clearly

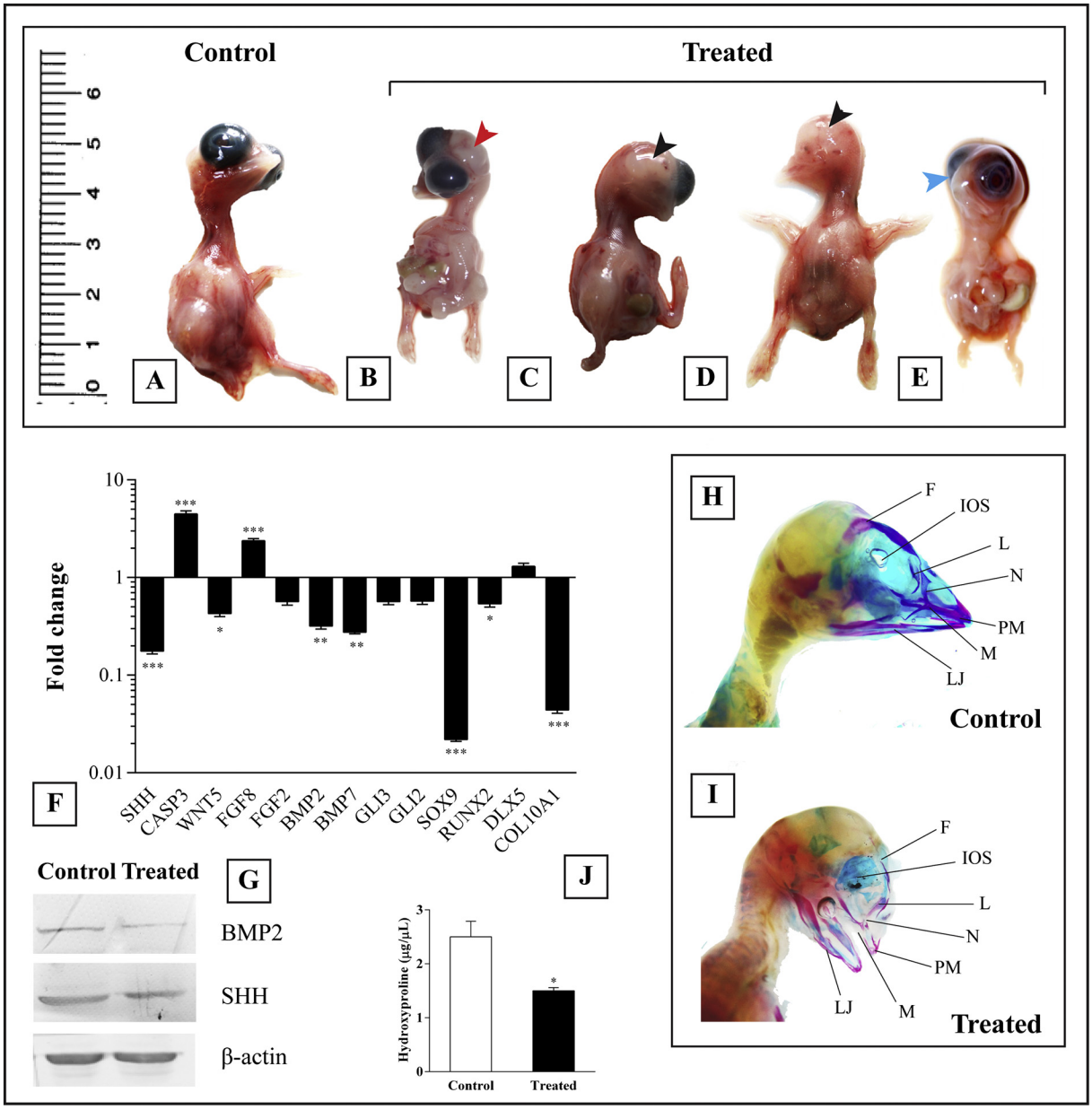

Fig. 3. Photograph of day 10 Control embryo with well-developed craniofacial structure (A); treated embryo indicating exposed brain marked by red arrowhead (B), phocomelia (C), anophthalmia marked by black arrowhead (C and D) and beak deformity shown by blue arrowhead (E). Scale in cm; (F) transcript levels of genes regulating chondrogenesis in Ci treated day 10 embryos: Values are expressed in fold change (Mean ± SEM). Fold change values for control embryo is 1.0 for all the genes (n = 3); (G) Western Blot images showing comparative expression of BMP2 and SHH on day 10. β-Actin was taken as loading control; embryos demonstrating differential staining of bone and cartilage in control (H) and treated (I) embryos respectively (F: frontal, IOS: interorbital septum, L: lachrymal, N: nasal, PM: premaxilla, M: maxilla, LJ: lower jaw); (J) Hydroxyproline content in control and treatment groups (n = 3) (*: $p \leq 0.05$; **: $p \leq 0.01$; ***: $p \leq 0.001$).

indicated roles in the development of eye structures (Solloway and Robertson, 1999). In the present study, the mRNA expression analysis on day 2 and 4 embryos showed a relatively downregulated expressions of SHH and BMP7 in Ci treated embryos. The reduction in SHH expression was evident even at protein level, and together with the observed reduction in the level of BMP7, this might be a contributing factor for the craniofacial deformities including the deviant development of eye noticed in Ci challenged embryos.

Another important family of signalling molecule, the WNTs is responsible for inducing proliferation in neural tube and thereby regulating multiple aspects of animal development and adult homeostasis (Megason and McMahon, 2002). One of the studies has shown the role of Wnt signals in the vertebrate nervous system for developing axonal guidance to synaptic region. In the developing vertebrate brain, WNT1, WNT5A and WNT7A are expressed with an overlapping spatiotemporal pattern and any alteration in this signalling pathway leads to craniofacial dysmorphism (Brault et al., 2001). Also, there are evidences suggesting that the WNTs are acting downstream of the BMPs (Wine-Lee et al., 2004). In the present study, the mRNA expression analysis on day 2 and 4 subjects showed that the Ci treated embryos had a downregulation of WNT1, WNT5A and WNT7A when compared to the control ones. This dysregulation in their expression might be the consequence of downregulated mRNA levels of BMP7, which must have further worsened neural tube development and the cell proliferation.

Moreover, neural crest (NC) cells are known to be involved in patterning the head and require a synchronized regulation of cell number to tissue size. This probably occurs through a combination of events like cell proliferation and survival which is controlled by SHH (Xavier et al.,

Table 6
Transcript levels of genes regulating chondrogenesis in Ci treated day 10 embryos. Fold changes are expressed as Mean ± SEM. Fold change values for control embryo is 1.0 for all the genes; n = 3 with 30 eggs per group per experiment.

Gene expression	Fold change (mean ± SEM)
SHH	0.176 ± 0.011***
CASPASE3	4.485 ± 0.320***
WNT5A	0.428 ± 0.031*
FGF8	2.378 ± 0.120***
FGF2	0.568 ± 0.047
BMP2	0.319 ± 0.022**
BMP7	0.276 ± 0.011**
GLI3	0.566 ± 0.038
GLI2	0.572 ± 0.041
SOX9	0.022 ± 0.001***
RUNX2	0.538 ± 0.041*
DLX5	1.301 ± 0.098
COL10A1	0.044 ± 0.003***

* $p \leq 0.05$.
** $p \leq 0.01$.
*** $p \leq 0.001$

Table 7
Spot densitometry analysis of the western blot bands on day 2, 4 and 10 embryos. The values are expressed as mean ± SEM; n = 3 with 30 eggs per group per experiment.

Protein	Band intensity in arbitrary units	
	Control	Treated
Day 2		
N-CADHERIN	88.16 ± 8.2	58.23 ± 5.5*
E-CADHERIN	40.25 ± 3.89	27.06 ± 2.4*
SHH	59.11 ± 5.98	27.52 ± 2.9**
PAX6	74.95 ± 7.24	45.91 ± 4.3*
B-ACTIN	96.44 ± 9.1	100.1 ± 10.12
Day 4		
CL.CASPASE3	23.55 ± 2.3	45.89 ± 3.52**
SHH	78.96 ± 7.96	43.26 ± 4.5*
B-ACTIN	114.99 ± 11.2	100 ± 10.1
Day 10		
BMP2	55.32 ± 4.23	27.56 ± 2.5**
SHH	82.88 ± 7.1	60.25 ± 5.23*
B-ACTIN	100 ± 8.3	99.3 ± 8.23

* $p \leq 0.05$.
** $p \leq 0.01$.

Table 8
Morphometry of the maximum horizontal breadth of the head of day 10 embryos. The values are expressed as Mean ± SEM; n = 3 with 30 eggs per group.

Group	Head breadth (mm) on day 10
Control	10.692 ± 0.09
Treated	8.372 ± 0.08****

**** $p \leq 0.001$.

2016). It can be hypothesized that diminished levels of SHH signalling hampers the growth of the neural tube, primarily because of increased cell death, which leads to an overall reduction in head size in the pesticide intoxicated embryos. We checked the levels of CASPASE3 and PCNA and found respective hike and fall in their mRNA levels, in treated embryos. The western blot analysis confirmed the reduction of CASPASE3 in the treated embryos. The decrease in head size could be an outcome of neural crest cell death and hence, it appears to be its primary determinant. In addition to the defects observed in the present study, we have noted occurrence of wavy neural tube due to intoxication of chlorpyrifos and cypermethrin in combination. This abnormality has been observed in mice with defects in platelet derived growth factor (PDGF) receptor, which is mediated through SHH (Suzuki et al., 2016).

The Sonic Hedgehog, through its downstream GLI zinc-finger transcriptional regulators, orchestrates two major functions - cell proliferation and patterning during the neurulation process. However, these factors appear to be absent during migration of cranial neural crest cells (Xavier et al., 2016). Moreover, Aoto et al. (2002) have documented the involvement of GLI3 in suppressing Fgf8 in the developing neural tube of mouse embryo. We have observed similar incidences of GLI3 downregulation, resulting in the upregulation of Fgf8 expression. Since FGF8 is essential for the control of pattern formation in the developing embryo, and as opined by Yardley and García-Castro (2012), its elevated expression can affect the developmental programs of many tissues.

Further, in the embryonic development, the neural tube undergoes drastic changes to attain anterior-posterior identity. Towards the anterior region, the neural tube organizes itself into three balloon like structures namely the prosencephalon, mesencephalon and the rhombencephalon. These primary vesicles differentiate into secondary structures i.e. forebrain that differentiates into telencephalon (forming the cerebral hemispheres) as well as the diencephalon (forming the optic vesicle for the development of eye), the midbrain which transforms into mesencephalon and the hindbrain which develops metencephalon as well as myelencephalon (Gilbert, 2003). The boundaries of these vesicles are marked by the presence of SHH and FGF8. Both these paracrine diffusible factors are also involved in patterning of CNC cells in the rostro-caudal manner. Several studies have supported the role of growth factors, including FGF, BMP and WNT as they regulate and define the positional identity of neural crest cells and their derivatives (Suzuki et al., 2016). FGF8, a member of FGF family, is reported to be involved in the neural crest induction, patterning, and its migration by upregulating the expression of various transcriptional factors (Yardley and García-Castro, 2012). FGF8 along with SHH marks the midbrain and hindbrain boundary, by silencing the HOX gene expression in the pre-migratory CNC cells (Irving and Mason, 2000). Several lines of evidence have also stated overexpression of Fgf8 leading to severe developmental defects in telencephalon, mesencephalon and pharyngeal arches (Martin and Kimelman, 2012; Shao et al., 2015). Cell patterning in the anterior most part of the brain requires low levels of FGF8 for induction of HOX10A and HOX11A which confers positional identity to CNC cells in the brain. In the present study, we observed an elevated expression of FGF8 which could be a plausible reason behind downregulation of HOX genes, resulting in poor development of telencephalon in pesticide treated embryos. Another study in mice showed heightened FGF8 expression and its activation by Wnt in the neural crest cells, which leads to severe craniofacial abnormalities, including exencephaly and anophthalmia (Prakash et al., 2006). Further, the levels of transcription factor PAX6, involved in migration of CNC cells, was evaluated. Pax6 is influenced by FGF to mediate morphogenesis of the CNC cell derivatives to form facial structures (Makarenkova et al., 2000). Normal expression of PAX6 is required to guide CNC cells migration for forebrain patterning. In the development of eye, role of Pax6 appears to be of prime importance in the communication between CNC cell derivatives, required for lens induction as well as for corneal and retinal development (Nelms and Labosky, 2010). The downregulated levels of PAX6 at mRNA and protein levels suggests its inefficiency at a reduced level to guide CNC cells to form optic stalk leading to absence of optic cup and causing anophthalmia in the pesticide treated embryos.

As described by Knight and Schilling (2013), neural crest cells are derived from the anterior most part of the neural plate and have the potential to form the skeletal tissue. In avian model system, little is known about the genetic regulation of cranial vault development. Most of the skeletal system undergoes endochondral ossification, to differentiate mesenchymal cells into chondrocytes, eventually leading to the

bone formation (Kronenberg, 2003). In the current study we have observed severely compromised chondrogenesis, especially in the craniofacial region of the chicks due to pesticide intoxication. To get insight into the extant of bone and cartilage formed by day 10 chick embryos, head region of control and treated groups were stained with Alcian blue and Alizarin red. The pesticide in question delayed the bone formation in the dosed group as compared to control. The cartilage formed was checked biochemically, by estimation of hydroxyproline. Hydroxyproline is the amino acid found in the highest concentration in collagen. This fibrous structural protein is abundantly seen in cartilage. During early embryogenesis, the skeletal system is made up of cartilage from mesenchymal tissue which further differentiates into chondrocytes and later replaced by endochondral ossification. The treated group embryos showed diminished level of hydroxyproline indicating less amount of cartilage formed as compared to control indicating the toxic manifestation of Ci.

There is substantial evidence to prove the role of BMPs in inducing bone formation and regulating chondrogenesis (Kamiya and Mishina, 2011). The use of genetically modified mice has unearthed various signalling pathways activated by BMPs that control multiple aspects of chondrogenesis (Kugler et al., 2015). Herein, we have chosen BMP2 and BMP7 for the study as they play a major role in chondrogenic and osteogenic differentiation. It was suspected that the Ci treatment might have hampered the BMP signalling and hence, hindered the process of cartilage formation and condensation. In order to test the above notion a mechanistic study, primarily focusing on the expression pattern of BMP2 and BMP7 was performed and the levels of both were found to be significantly downregulated in the pesticide treated embryos. The bone morphogenetic proteins target transcription factors that induce differentiation of mesenchymal cells towards ossification in which SOX9 and RUNX2, are important. SOX9 is a chondrocyte marker expressed during early differentiation stages. Gene expression studies in mouse have established the role of SOX9 in activating chondrocyte-specific markers such as COL10A1, COL2A1 and Aggrecan to form cartilage (Shen et al., 2010). On the other side, to differentiate chondrocytes into osteoblasts, a member of the runt homology domain factor RUNX2 is required. Also, its expression is suggested to be causing proliferation of osteoblast progenitors and thus regulating the first check point of chondrocyte maturation to osteoblasts (Shen et al., 2010). The analysis of the result revealed significant downregulation of mRNA expression levels of RUNX2, SOX9 as well as COL10A1 and reduction in protein level expression of one of their upstream modulators named BMP2 upon combination insecticide treatment. This points to a possible derailment of SOX9 and RUNX2 signalling pathway in treated embryos, and hence might have caused impromptu sculpting of the head and facial structures.

The cranial vault in the chick embryo forms almost entirely by the endochondral ossification. DLX5, a transcription factor from distal-less, homeodomain-containing family is expressed before osteoblast differentiation and in proliferating osteoblast precursors and is required for craniofacial morphogenesis (Holleville et al., 2003). It is mainly expressed during the formation of structural elements such as cartilage. DLX5 null mutations in mice have testified its part in triggering skeletal defects in the form of deferred endochondral ossification and abnormal osteogenesis. Knockout studies have reported craniosynostosis syndromes and severed chondrogenesis (Holleville et al., 2003). Herein, pesticide intoxication led to high levels of DLX5 expression in the treated embryos. Heightened expression of DLX5 impairs differentiation of chondrogenic precursors into osteoblasts of humans. Dlx5 transcription in the current study, might have been upregulated by BMP4 and BMP7 when expressed together.

Another major factor in skeletal development is the expression of WNTs, which are crucial signals for regulation of chondrocyte and osteoblast differentiation (Day and Yang, 2008). Wnt5a is involved in pattern formation along the AP axis by regulation of chondrogenic differentiation through SOX9. On the contrary, it suppresses hypertrophic chondrocytes by inhibiting RUNX2 expression (Bradley and Drissi, 2010). The pesticide treated embryos showed downregulation of WNT5A expression, thereby inhibiting the formation of chondrocytes by significantly suppressing the expression of SOX9.

It is well established that BMP2 plays a critical role in osteoblast function mediating its activity through hedgehog signalling. Gli proteins play an essential role as transcriptional activator (GLI2) and repressor (GLI3) in embryonic development by regulating SHH target genes. Null mutation of GLI2 in mice has caused structural defects. Sonic hedgehog stimulates BMP2 activity in osteoblast differentiation and the effects of SHH are mediated by Gli2 (Zhao et al., 2006). In the present study, we observed reduction in mRNA as well as protein levels of SHH and subdued mRNA levels of GLI2, affecting further expression of BMP2 and its downstream effectors. Both the signals together indicate their expression to be a powerful activator of BMP2 expression required for normal osteoblast differentiation. Gli3, a transcriptional repressor of SHH pathway, also has been reported to trigger skeletal defects in mice and humans (Yip et al., 2019). Downregulated levels of GLI3 observed in the current study support the concept of FGF8 overexpression, causing abnormal apoptosis of the skeletal tissues. A similar report wherein defects in GLI3 and FGF8 signalling causing neural tube related defects in mice (Putoux et al., 2018) further consolidates the veracity of the present observation.

The study was further extended to understand the role of FGFs in skeletal development wherein FGF2 and FGF8 are the major candidates. The results vividly expressed that pesticide treatment induced downregulation of BMP2 and BMP7, possibly as a result of the increased expression of Fgf8 which is known to antagonize the action of BMP (Yoon and Lyons, 2004). Moreover, it has been documented that the upregulated expression of Fgf8 will activate the apoptotic pathway (Wan and Cao, 2005). To ascertain the extent of cell death, day 10 chick embryos were extracted, and CASPASE3 activity was checked. It was observed that CASPASE3 activity increased progressively by several times in treated group compared to the control group embryos. Overall, it showed an unusual pattern of apoptosis due to diminished BMP signalling in treated groups. Kawane et al. (2018) have elaborated the role of FGF signalling in skeletal development, craniosynostosis, and the progression of some breast cancers. The osteoblast differentiation and proliferation of osteoblast progenitors requires a positive signal from RUNX2 (as discussed earlier) and fibroblast growth factor 2 enhances its ability through MAPK pathway. However, quite contrary to this, in Ci treated embryos the level of RUNX2 remained low even though FGF2 showed significant upregulation at transcript and protein levels. Similar result was reported by Moore et al. (2002) wherein elevated levels of FGF2 were localised in the undifferentiated mesenchyme around the bones in the embryonic tissue of chick. These results suggest that other factors must be acting upstream of Runx2 in controlling osteogenesis and chondrogenesis. And conclusively, our observations when monitored at microlevel could be connected to not just isolated signalling molecules but too many of such regulatory molecules, which sets an alarm on how devastating a toxic exposure during the phase of embryonic development could be and that the process of development which does not stop with the embryonic phase and happens throughout the animal life.

5. Conclusion

The pesticide treated embryos showed various congenital malformations in the head region due to aberrant mRNA expressions of the regulatory signals of the cellular processes like cell migration, differentiation, proliferation and survival. We observed defects in the closure of neural tube that form the craniofacial cartilage. Also, incoherent chondrogenesis was noted in the cranial vault. The development of head is under intricate control of the regulatory signal, rely on constant inter-communication between the morphogens and the surrounding tissues that displayed erroneous results due to pesticide intoxication.

Because of the reduced levels of cell adhesion molecules and major regulatory signals like SHH, BMP7, FGF8, the neural tube failed to close and morphogenetic movements were affected. In the later development, the neural tube failed to pattern the tissues to form telencephalon along with other brain vesicles. The failure in cell migration process leads to the absence of eye stalk on day 2 which added clues in occurrence of anophthalmia on day 4. The toxic manifestations of the pesticides were later seen in the developing embryos (day 10) where the cranial structures were unsuccessful to differentiate and ossify. These abnormal cranial structures were the derivatives of neural crest cell derived mesenchymal cells that underwent impromptu signalling at early stages. The pesticide dosed embryos thus faced a grave consequence in achieving their cell fate due to the possible derailment in the expression pattern of the supervisory signals which ultimately led to the craniofacial dysmorphism.

Acknowledgement and funding information

The authors are grateful to Department of Science and Technology-Science and Engineering Research Board (Grant number: SB/SO/AS-008/2014), New Delhi for financial assistance in the form of a major research project sanctioned to SB.

Declaration of competing interest

The authors declare that they have no known competing financial interests or personal relationships that could have appeared to influence the work reported in this paper.

References

Abdul-Ghani, S., Yanai, J., Abdul-Ghani, R., Pinkas, A., Abdeen, Z., 2012. The teratogenicity and behavioral teratogenicity of di (2-ethylhexyl) phthalate (DEHP) and di-butyl phthalate (DBP) in a chick model. Neurotoxicol. Teratol. 34, 56–62.
Ahlgren, S.C., Bronner-Fraser, M., 1999. Inhibition of sonic hedgehog signaling in vivo results in craniofacial neural crest cell death. Curr. Biol. 9, 1304–1314.
Ahmed, K.R., 2007. Asmatullah, Teratological effects of chlorpyrifos in mice. Iranian J. Toxicol 1, 91–99.
Aoto, K., Nishimura, T., Eto, K., Motoyama, J., 2002. Mouse GLI3 regulates Fgf8 expression and apoptosis in the developing neural tube, face, and limb bud. Dev. Biol. 251, 320–332.
Blankenship, A.L., Hilscherova, K., Nie, M., Coady, K.K., Villalobos, S.A., Kannan, K., ... Giesy, J.P., 2003. Mechanisms of TCDD-induced abnormalities and embryo lethality in white leghorn chickens. Comp Biochem Physiol PT C 136, 47–62.
Bradford, M.M., 1976. A rapid and sensitive method for the quantitation of microgram quantities of protein utilizing the principle of protein-dye binding. Anal. Biochem. 72 (1–2), 248–254.
Bradley, E.W., Drissi, M.H., 2010. WNT5A regulates chondrocyte differentiation through differential use of the CaN/NFAT and IKK/NF-κB pathways. Molecular Endocrinol 24, 1581–1593.
Brault, V., Moore, R., Kutsch, S., Ishibashi, M., Rowitch, D.H., McMahon, A.P., ... Kemler, R., 2001. Inactivation of the (β)-catenin gene by Wnt1-Cre-mediated deletion results in dramatic brain malformation and failure of craniofacial development. Development 128, 1253–1264.
Centers for Disease Control and Prevention, 2012. National center on birth defects and developmental disabilities. Promoting the health of babies, children, and adults and enhancing the potential for full, productive living. In: Annu Rep, Fiscal Year.
Day, T.F., Yang, Y., 2008. Wnt and hedgehog signaling pathways in bone development. JBJS 90, 19–24.
Depew, M.J., 2008. Analysis of skeletal ontogenesis through differential staining of bone and cartilage. In: Mol Embryol, pp. 37–45.
Detrick, R.J., Dickey, D., Kintner, C.R., 1990. The effects of N-cadherin misexpression on morphogenesis in Xenopus embryos. Neuron 4, 493–506.
Edwards, C.A., O'Brien Jr., W.D., 1980. Modified assay for determination of hydroxyproline in a tissue hydrolyzate. Clin. Chim. Acta 104, 161–167.
Fish, J.L., 2016. Developmental mechanisms underlying variation in craniofacial disease and evolution. Develop Biol 415, 188–197.
Gilbert, S.F., 2003. The morphogenesis of evolutionary developmental biology. International J Dev Biol 47, 467.
Griffin, J.N., Compagnucci, C., Hu, D., Fish, J., Klein, O., Marcucio, R., Depew, M.J., 2013. Fgf8 dosage determines midfacial integration and polarity within the nasal and optic capsules. Dev. Biol. 374, 185–197.
Hamburger, V., Hamilton, H.L., 1951. A series of normal stages in the development of the chick embryo. J. Morphol. 88, 49–92.
Holleville, N., Quilhac, A., Bontoux, M., élène Monsoro-Burq, A.H., 2003. BMP signals regulate Dlx5 during early avian skull development. Dev. Biol. 257, 177–189.
Irving, C., Mason, I., 2000. Signalling by FGF8 from the isthmus patterns anterior hindbrain and establishes the anterior limit of Hox gene expression. Development 127, 177–186.
Kalliora, C., Mamoulakis, C., Vasilopoulos, E., Stamatiades, G.A., Kalafati, L., Barouni, R., ... Tsatsakis, A., 2018. Association of pesticide exposure with human congenital abnormalities. Toxicol. Appl. Pharmacol. 346, 58–75.
Kamiya, N., Mishina, Y., 2011. New insights on the roles of BMP signaling in bone—a review of recent mouse genetic studies. Biofactors 37, 75–82.
Kawane, T., Qin, X., Jiang, Q., Miyazaki, T., Komori, H., Yoshida, C.A., ... Maeno, T., 2018. Runx2 is required for the proliferation of osteoblast progenitors and induces proliferation by regulating Fgfr2 and Fgfr3. Sci. Rep. 8, 13551.
Knight, R.D., Schilling, T.F., 2013. Cranial neural crest and development of the head skeleton. In: Madame Curie Bioscience Database [Internet]. Landes Bioscience.
Kronenberg, H.M., 2003. Developmental regulation of the growth plate. Nature 423, 332.
Kugler, J., Tharmann, J., Chuva de Sousa Lopes, S.M., Kemler, R., Luch, A., Oelgeschläger, M., 2015. A Bmp reporter transgene mouse embryonic stem cell model as a tool to identify and characterize chemical teratogens. Toxicol. Sci. 146, 374–385.
Livak, K.J., Schmittgen, T.D., 2001. Analysis of relative gene expression data using real-time quantitative PCR and the $2-\Delta\Delta CT$ method. METHODS 25 (4), 402–408.
Makarenkova, H.P., Ito, M., Govindarajan, V., Faber, S.C., Sun, L., McMahon, G., ... Lang, R.A., 2000. FGF10 is an inducer and Pax6 a competence factor for lacrimal gland development. Development 127, 2563–2572.
Martin, B.L., Kimelman, D., 2012. Canonical Wnt signaling dynamically controls multiple stem cell fate decisions during vertebrate body formation. Dev. Cell 22, 223–232.
Mayor, R., Theveneau, E., 2013. The neural crest. Development 140, 2247–2251.
Megason, S.G., McMahon, A.P., 2002. A mitogen gradient of dorsal midline Wnts organizes growth in the CNS. Development 129, 2087–2098.
Moore, R., Ferretti, P., Copp, A., Thorogood, P., 2002. Blocking endogenous FGF-2 activity prevents cranial osteogenesis. Dev. Biol. 243 (1), 99–114.
Nelms, B.L., Labosky, P.A., 2010. Transcriptional control of neural crest development. Dev. Biol. 1, 1–227.
Nikolopoulou, E., Galea, G.L., Rolo, A., Greene, N.D., Copp, A.J., 2017. Neural tube closure: cellular, molecular and biomechanical mechanisms. Development 144, 552–566.
Prakash, N., Brodski, C., Naserke, T., Puelles, E., Gogoi, R., Hall, A., ... Martinez, S., 2006. A Wnt1-regulated genetic network controls the identity and fate of midbrain-dopaminergic progenitors in vivo. Development 133, 89–98.
Putoux, A., Baas, D., Paschaki, M., Morlé, L., Maire, C., Attié-Bitach, T., ... Durand, B., 2018. Altered GLI3 and FGF8 signaling underlies Acrocallosal syndrome phenotypes in Kif7 depleted mice. Hum. Mol. Genet. 28, 877–887.
Ray, D.E., Forshaw, P.J., 2000. European association of poison centres and clinical toxicologists xix international congress pesticide symposium-Pyrethroid Insecticides: Poisoning Syndromes, Synergies, and Therapy-The poisoning. Journal of Toxicology-Clinical Toxicology 38, 95–102.
Sawad, A.A., Hana, B.A., Al-Silawi, A.N., 2009. Morphological study of the skeleton development in chick embryo (Gallus domesticus). Int J Poul Sci 8, 710–714.
Shao, M., Liu, C., Song, Y., Ye, W., He, W., Yuan, G., ... Tian, W., 2015. FGF8 signaling sustains progenitor status and multipotency of cranial neural crest-derived mesenchymal cells in vivo and in vitro. J. Mol. Cell Biol. 7, 441–454.
Sharma, S., Uggini, G.K., Patel, V., Desai, I., Balakrishnan, S., 2018. Exposure to sub-lethal dose of a combination insecticide during early embryogenesis influences the normal patterning of mesoderm resulting in incomplete closure of ventral body wall of chicks of domestic hen. Tox Rep 5, 302–308.
Shen, B., Wei, A., Whittaker, S., Williams, L.A., Tao, H., Ma, D.D., Diwan, A.D., 2010. The role of BMP-7 in chondrogenic and osteogenic differentiation of human bone marrow multipotent mesenchymal stromal cells in vitro. J. Cell. Biochem. 109, 406–416.
Slotkin, T.A., Ryde, I.T., Levin, E.D., Seidler, F.J., 2008. Developmental neurotoxicity of low dose diazinon exposure of neonatal rats: effects on serotonin systems in adolescence and adulthood. Brain Res. Bull. 75, 640–647.
Solloway, M.J., Robertson, E.J., 1999. Early embryonic lethality in Bmp5; Bmp7 double mutant mice suggests functional redundancy within the 60A subgroup. Development 126, 1753–1768.
Suzuki, A., Sangani, D.R., Ansari, A., Iwata, J., 2016. Molecular mechanisms of midfacial developmental defects. Develop Dynam 245 (3), 276–293.
Taneyhill, L.A., 2016. Neural crest-placode cell interactions during cranial ganglia assembly. FASEB J. 30 (8-3).
Uggini, G.K., Suresh, B., 2013. Genotoxic effects of two different classes of insecticide in developing chick embryos. Environ. Toxicol. Chem. 95, 992–1005.
Uggini, G.K., Patel, P.V., Balakrishnan, S., 2012. Embryotoxic and teratogenic effects of pesticides in chick embryos: a comparative study using two commercial formulations. Environ. Toxicol. 27, 166–174.
Wan, M., Cao, X., 2005. BMP signaling in skeletal development. Biochem. Biophys. Res. Commun. 328, 651–657.
Wang, S., Garcia, M.D., Lopez, A.L., Overbeek, P.A., Larin, K.V., Larina, I.V., 2017. Dynamic imaging and quantitative analysis of cranial neural tube closure in the mouse embryo using optical coherence tomography. Biomed Opt Express 8, 407–419.
Wilde, J.J., Petersen, J.R., Niswander, L., 2014. Genetic, epigenetic, and environmental contributions to neural tube closure. Annu. Rev. Genet. 48, 583–611.
Wine-Lee, L., Ahn, K.J., Richardson, R.D., Mishina, Y., Lyons, K.M., Crenshaw, E.B., 2004. Signaling through BMP type 1 receptors is required for development of interneuron cell types in the dorsal spinal cord. Development 131, 5393–5403.
Xavier, G.M., Seppala, M., Barrell, W., Birjandi, A.A., Geoghegan, F., Cobourne, M.T., 2016. Hedgehog receptor function during craniofacial development. Dev. Biol. 415, 198–215.
Yang, L.M., Ornitz, D.M., 2019. Sculpting the skull through neurosensory epithelial–mesenchymal signaling. Develop Dynam 248, 88–97.

Yardley, N., García-Castro, M.I., 2012. FGF signaling transforms non-neural ectoderm into neural crest. Dev. Biol. 372, 166–177.
Yip, R.K., Chan, D., Cheah, K.S., 2019. Mechanistic insights into skeletal development gained from genetic disorders. Curr. Top. Dev. Biol. 133, 343–385.
Yoon, B.S., Lyons, K.M., 2004. Multiple functions of BMPs in chondrogenesis. J. Cell. Biochem. 93, 93–103.
Zhao, M., Qiao, M., Harris, S.E., Chen, D., Oyajobi, B.O., Mundy, G.R., 2006. The zinc finger transcription factor Gli2 mediates bone morphogenetic protein 2 expression in osteoblasts in response to hedgehog signaling. Mol. Cell. Biol. 26, 6197–6208.